



# SHAPE OPTIMIZATION OF UNCONSTRAINED VISCOELASTIC LAYERS USING CONTINUUM FINITE ELEMENTS

A. LUMSDAINE

*Mechanical Engineering Department, University of Texas-Pan American,  
1201 West University Drive, Edinburg, TX 78539, U.S.A.*

AND

R. A. SCOTT

*Department of Mechanical Engineering and Applied Mechanics, University of Michigan,  
G044 Auto Lab, Ann Arbor, MI 48109, U.S.A.*

*(Received 26 August 1997, and in final form 16 March 1998)*

Of the many methods available for achieving effective vibration damping, adding viscoelastic lamina is a significant technique for vibration reduction. Recently, the desire to apportion this material in a way that will take the greatest advantage of its dissipative characteristics has led to studies in optimization. Optimal design for viscoelastically damped laminated beams and plates undergoing harmonic excitation has been examined in the literature, both for constrained and unconstrained damping layers. However, to the authors' knowledge, previous optimization studies have not used continuum based finite elements to model the structure, as is done here. The problem examined is the shape optimization of an unconstrained damping layer on an elastic structure, assuming a constant volume of damping material as a design constraint. The objective is to minimize the peak displacement. Several boundary conditions are examined for beam and plate type structures. The peak displacement and the loss factor of the optimized structure are compared with the uniform layer structure. Also, results obtained using realistic (frequency dependent) and constant viscoelastic material data are compared. The structures are modelled using continuum based elements in the ABAQUS Finite Element Code. The optimization code uses a Sequential Quadratic Programming algorithm. For most of the structures examined, order of magnitude improvement is seen as a result of optimizing the shape of the damping layer. Peak displacements are reduced by up to 98%. These results are quite robust, with the optimized damping layer achieving significantly better damping performance for a wide variety of cases examined.

© 1998 Academic Press

## 1. INTRODUCTION

Of the many techniques available for reducing excessive vibrations, adding damping laminates is significant for many structures (see, for example, references [1–3]). These laminated damping treatments exist in two forms, constrained and unconstrained. In unconstrained layer damping, a viscoelastic damping layer is fixed to an elastic base structure, so that energy dissipation occurs in extension. In constrained layer damping, an additional elastic layer (which has an elastic modulus much higher than that of the damping layer) is placed on the damping layer so that energy dissipation occurs in shearing.

Useful methods for analysis of unconstrained and constrained damped laminated structures were developed by Ross *et al.* [4]. This work led to numerous studies, some of which are reviewed by Nakra [1–3]. Finite elements have frequently been employed to characterize the laminated structure (for example, reference [5]).

More recently, the desire to apportion this material in a way that will take the greatest advantage of its dissipative characteristics has led to studies in optimization. The work up till now has employed structural theories. Plunkett and Lee [6] optimized constraining layer tape lengths on beams in order to maximize the system loss factor. Lundén [7, 8] optimized the heights of the constrained damping layer on a beam and on vibrating frames. Lekszycki and Olhoff [9] optimized the shape of an unconstrained damping layer on a beam structure using variational techniques. Pierson [10] performed the same analysis as Lekszycki and Olhoff by means of an optimal control approach. Yildiz and Stevens [11] optimized unconstrained damping layer heights on a plate. Lin and Scott [12] optimized the shape of a damping layer for both constrained and unconstrained beams, developing their own finite element code to model the structure. Lifshitz and Leibowitz [13] maximized the system loss factor of a constrained layer beam with respect to the stiffnesses and heights of all three layers. All layers are of uniform height in this case. The beam was modelled using the sixth order differential equations developed by Mead and Markus [14]. Hajela and Lin [15] used a global optimization strategy to maximize the system loss factor with respect to damping layer lengths for a constrained layer beam. They developed a finite element code and found the system loss factor by the Modal Strain Energy Method. Roy and Ganesan thoroughly examined partial damping layers for an unconstrained plate [16], and an unconstrained beam [17], modelling with finite elements. Lumsdaine and Scott [18] optimized the shape of an unconstrained damping layer using structural plate elements for modelling. However, to the authors' knowledge, previous optimization studies (both for constrained and unconstrained layers) have not used continuum based finite elements for modelling. A goal of this study is to determine the optimal shape of an unconstrained damping layer on an elastic structure, modelled with continuum based finite elements. Several of the above optimization studies (for example, references [11, 16, 17]) made the common assumption that the viscoelastic material properties are constant with frequency. Another goal of this study is to examine the consequences of that assumption on the results of optimization for cases where the material properties vary significantly with frequency.

The design objective is to minimize the midpoint displacement at the first resonant frequency of an unconstrained layer laminate, harmonically excited at its midpoint. The system loss factor is not taken as a design objective *per se*, but is monitored, and generally shows improvement of the same order of magnitude as the peak displacement at the midpoint. Six different structures are considered. Three boundary conditions (simply supported beam, simply supported plate, and fully clamped plate) are examined. Two different geometries (a “thin” structure and a “thick” structure) are examined for each constraint condition.\*

## 2. MODELLING

The unconstrained layer structures analyzed in this study are modelled with continuum based finite elements, using the commercial finite element code ABAQUS. ABAQUS also has a composite shell element within its element library. The CPU time required to obtain the finite element solution is much less for these shell elements than for continuum elements (by an order of magnitude), and so shell elements would seem to be a better choice for

\* Note that some of this work was presented at conferences [19, 20].

modelling the structure. However, it has been found that these elements have some limitations, and should be used with care. Figure 1 compares the system loss factors for plate and solid elements for various values of the base beam height. (ABAQUS version 5.3 was used to obtain these results.) The loss factor is plotted against the height of the damping layer ( $h_v$ ), normalized by the height of the base beam ( $h_b$ ) for a beam 178 mm in length ( $L$ ) and 25.4 mm in width. In all cases examined, the system loss factor is found at the first damped resonance frequency. All of the finite element models have converged.

It is clear that the range of validity for the plate elements is narrow. There is close agreement between the plate element and the solid element results for  $h_b = 1.52$  mm, where the aspect ratio (defined here as  $L/h_b$ ) is over 115. However, the results diverge significantly for  $h_b = 5.08$  mm (aspect ratio of 35). This is a surprising result, as this is a case where one would expect structural theory to be accurate. It can be concluded from these results that the composite structural elements in ABAQUS should be used with care. (Further studies may be found in reference [21]). In cases where the moduli of the materials in the composite differ significantly, ABAQUS plate elements should only be used when the entire structure is very thin, or the damping layer is very thin relative to the base layer. As these conditions are violated in many of the cases studied below, composite plate elements are inappropriate. Thus, quadratic continuum elements (20-noded for the elastic structures and 27-noded for the viscoelastic structures) are used for modelling. The reasons for using 27-noded elements for modelling the viscoelastic structure are detailed in the section 3 below.

The viscoelastic properties are modelled as follows. For a linear isotropic viscoelastic material harmonically forced at frequency  $\omega$ , the elastic modulus and shear modulus may be written as

$$E^*(\omega) = E_1(\omega) + iE_2(\omega), \quad G^*(\omega) = G_1(\omega) + iG_2(\omega). \quad (1, 2)$$

Equation (2) may also be written as

$$G^*(\omega) = G_1(\omega)[1 + i\eta_m(\omega)]. \quad (3)$$

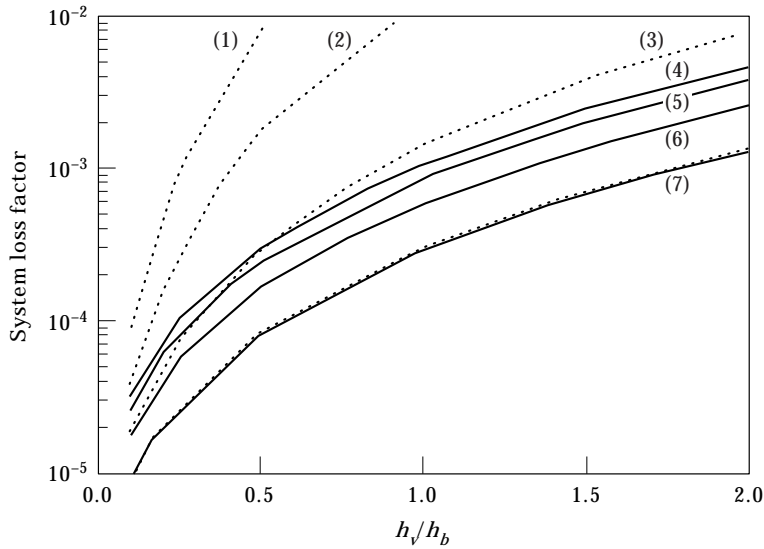


Figure 1. Comparison of system loss factors using plate (—) and solid (····) elements.  $h_b$  values for curves as follows: (1) 15.20 mm; (2) 10.20 mm; (3) 5.08 mm; (4) 15.20 mm; (5) 10.20 mm; (6) 5.08 mm; (7) 1.52 mm.

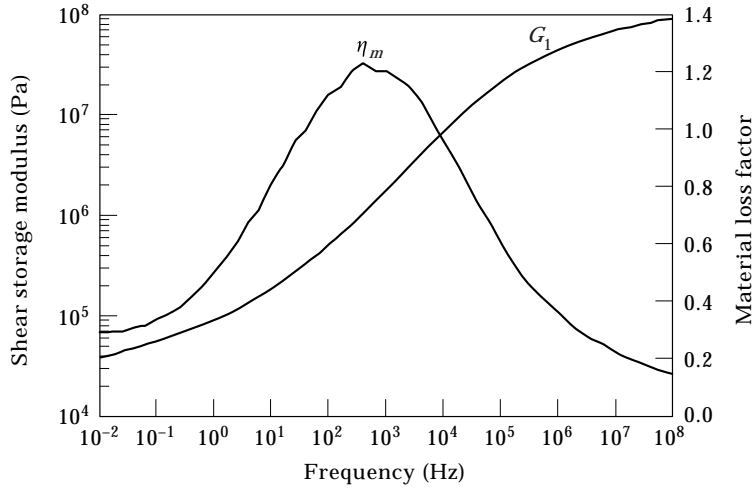


Figure 2. Shear storage modulus and material loss factor for damping material.

Here  $E_1$ ,  $E_2$ ,  $G_1$  and  $G_2$  denote the storage and loss moduli for extension and shear, respectively, and  $\eta_m$  is the material loss factor. In the sequel, the frequency dependence of these and other material properties will not be explicitly noted.

The complex bulk modulus is given by

$$K^* = K_1 + iK_2 = \frac{E^*}{3(1 - 2\nu^*)}, \quad (4)$$

where “ $\nu^*$ ” is the complex Poisson ratio defined through

$$G^* = \frac{E^*}{2(1 + \nu^*)}. \quad (5)$$

Viscoelastic properties can be entered into ABAQUS in several ways. In the frequency domain, tabular values of  $G_1$ ,  $G_2$ ,  $K_1$ , and  $K_2$ , suitably normalized, can be entered as functions of frequency. The dynamic elastic modulus and Poisson ratio may be related to the dynamic shear modulus and bulk modulus in the same way that the equivalent static properties are related. Thus, a dynamically varying Poisson ratio may be taken into account in entering the shear and bulk moduli.

The damping material properties used for this study were obtained from the 3M Corporation. (The material name and designation were not given, but the material properties are typical of the damping tapes produced by 3M). Figure 2 shows values of  $G_1$  and  $\eta_m$  as functions of frequency for this material.

Data for the Poisson ratio were not available from 3M. In fact, very little Poisson ratio data is available for viscoelastic materials in general. Often, viscoelastic materials are assumed to be incompressible ( $\nu = 0.5$ ) in regions of rubbery behavior (low frequencies/high temperatures), and about 0.3 in regions of glassy behavior (high frequencies/low temperatures). The fact that the Poisson ratio varies with frequency, temperature, and strain magnitude is well documented (see, for example, reference [22]). The measurement of this variation is very difficult to obtain experimentally, however, and is not available for most damping materials. The operating frequencies examined in this study range between 100 and 1300 Hz. As is clear in Figure 2, this is in the damping material’s transition region. In the absence of any specific data for this material, a constant

Poisson ratio of 0.4 (between 0.3 and 0.5) is assumed. Aluminum is used as the material for the base layer. Material properties are listed in Table 1.

An important parameter for measuring the amount of damping energy lost in a harmonically vibrating structure is the system loss factor, which is exactly defined by [23]

$$\eta = \frac{\omega_1^2 - \omega_2^2}{2\omega_d^2}, \quad (6)$$

where  $\omega_1$  and  $\omega_2$  are the frequencies at the half power points and  $\omega_d$  is the damped natural frequency. In cases where the damping is light, equation (6) reduces to

$$\eta = (\omega_1 - \omega_2)/\omega_d, \quad (7)$$

which is the familiar form of the system loss factor. The system loss factor will be calculated and used for monitoring the improvement in damping performance for the optimal designs. As some results give very high loss factors, the exact definition (equation (6)) is used.

### 3. OPTIMIZATION METHODOLOGY

The range of possible optimization strategies available in structural optimization is limited by the structural modelling. For instance, variational techniques together with analytical methods are available for optimizing the shape of continuous media, but not for optimizing the shape of a structure which has been discretized. Since the structures optimized here are modelled using finite elements, the optimization strategies are limited by the discretization process. Quadratic continuum elements (20- or 27-noded) are used for modelling. There are many possible design variable selections using quadratic elements. As each of the eight faces of the solid may be defined as a quadratic surface, these elements allow significant latitude in the modelling of the structure. One possibility for modelling would be to define the top surface of the damping layer as a series of cubic splines. The spline curve coefficients would be the design variables in this case. Then, using a node generation algorithm to determine the number and the placement of the elements, an entirely new mesh would be generated with each new design. The most general application of this would include the possibility that several elements be allowed through the thickness of the damping layer. However, beyond the complexity involved in developing such an algorithm and integrating it with a commercial code, this approach would require a significantly larger number of elements than if just one layer of elements for the damping material were allowed. As the optimization process may involve hundreds of finite element runs, the time required by this approach would be computationally excessive. Thus, only one element through the thickness is used for the damping layer. It is believed that this will capture the essential features of the damping layer behavior. Fine mesh validation models are developed for both the uniform layer and optimized shapes to confirm this.

TABLE 1  
*Material properties*

	Aluminum	Damping material
Density (kg/m <sup>3</sup> )	2800	970
Elastic moduli (Pa)	$6.9 \times 10^{10}$	See Figure 2
Poisson's ratio	0.3	0.4

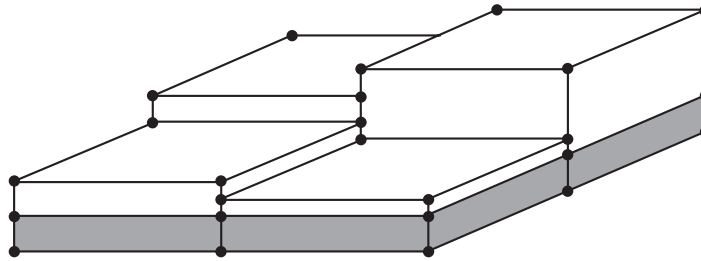


Figure 3. Optimization using element heights as design variables.

Several possibilities were examined for design variable selection. Many of them led either to unacceptable geometric complexity or to a model requiring too many elements, which would result in excessive CPU time (see reference [21]). It was decided that the damping layer elements would be held to a constant height, and that the heights of the damping material elements would be the most appropriate choice for the design variables.

This choice of design variables also has some difficulties, however. As can be seen in Figure 3 (which shows 8-noded continuum elements for simplicity), nodes of adjacent damping layer elements are not all coincident. Thus, multi-point constraints (MPCs) are necessary in order to enforce displacement continuity of adjacent elements. Multi-point constraints are a means of defining the degrees of freedom at a node (or set of nodes) by relating them to the degrees of freedom of a different set of nodes. This is most conveniently done using the ABAQUS 27-noded continuum element. The 27-noded element is identical to the 20-noded element except that additional nodes are defined at the center of the element, and at the center of each face. The following describes how these MPCs are applied.

Adjacent faces of two sets of elements are shown in Figure 4. ABAQUS has a quadratic MPC capability, where the degrees of freedom for a given node can be constrained to lie on a quadratic curve defined by three other nodes. Thus, referring to Figure 4, the MPCs

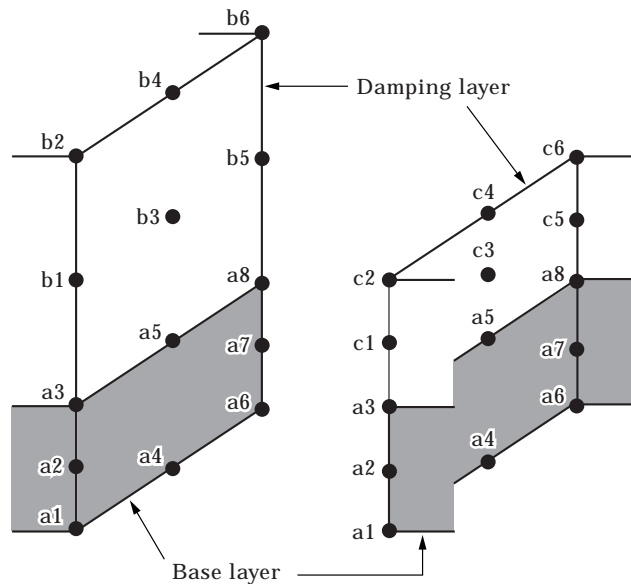


Figure 4. Exploded view of adjacent elements.

are assigned as follows: nodes c1 and c2 are constrained to lie on the curve defined by nodes a3–b1–b2; nodes c3 and c4 are constrained to lie on the curve defined by nodes a5–b3–b4; nodes c5 and c6 are constrained to lie on the curve defined by nodes a8–b5–b6. Another possibility is to assign the MPCs in the opposite direction, as follows: nodes b1 and b2 are constrained to lie on the curve defined by nodes a3–c1–c2; nodes b3 and b4 are constrained to lie on the curve defined by nodes a5–c3–c4; nodes b5 and b6 are constrained to lie on the curve defined by nodes a8–c5–c6. The same results are obtained regardless of which direction the MPC are assigned.

It should be emphasized that for every structure studied, the values for the damped resonance frequency, the peak displacement, and the loss factor of the optimal shape are confirmed by an independent, fine mesh, validation model. Compatibility between adjacent elements is enforced in the validation model just as in the optimization model, except that nodes are shared by adjacent elements, so that multi-point constraints are unnecessary.

A standard code was used for the optimization, which uses an SQP (Sequential Quadratic Programming) algorithm. For details on the algorithm and the code used (NLPQL), see Schittkowski [24]. Optimization requires a technique for finding the gradient of the objective function with respect to the design variables. Finding analytical gradients is an extremely complex task for a problem of this scope, so gradients are calculated numerically by a finite difference method.

Now, consideration will be given to the selection of the objective function. Often, in structural problems, the objective is to maximize the lowest eigenvalue (natural frequency) of the structure. For damped laminated structures, the objective function is usually either a global measure of energy dissipation, such as the loss factor, or a local measure, such as the peak displacement (see reference [25] for an examination of both measures). For a structure where energy is dissipated by viscous damping, minimizing the peak displacement would be a dual problem to maximizing the loss factor; that is all else being equal, these two objectives would yield the same solution. However, for frequency dependent damping, such as is present in damped laminated composites, this is not always the case, as was demonstrated by Lall *et al.* [25].

Since different solutions could be found depending on whether the performance measure is the loss factor or the peak displacement, it must be considered which measure would have greater merit and ease of use in the problem at hand. Since the loss factor is a global measure, it would seem to be a more robust measure of the composite's performance. However, calculating the loss factor by the half power bandwidth requires calculating results at many points in a given frequency range, which, in turn, requires a lengthy finite element calculation. The disk space required for these large calculations also become prohibitive. Thus, using peak displacement as the measure of performance is an attractive alternative, in that it does not have these same computational requirements. The loss factor is monitored, however, and shows improvement similar to that of the peak displacement for the optimal design in every case.

Minimizing the peak displacement requires finding the new resonance peak with each structural change. After each design change, a frequency response curve is generated over a large frequency band. The location of the peak displacement in this curve dictates the choice of a new, narrower band. This process continues until the desired precision of the displacement is achieved.

The physical constraints used in this problem are as follows. A lower bound is placed on the height of the viscoelastic layer for each element in order to maintain the integrity of the finite element. This was set to be 0.254 mm in all cases, so that the element aspect ratios would not exceed 100. An upper bound is set on the volume of the damping material. This is set to be the volume of the base layer. A design constraint is added to take

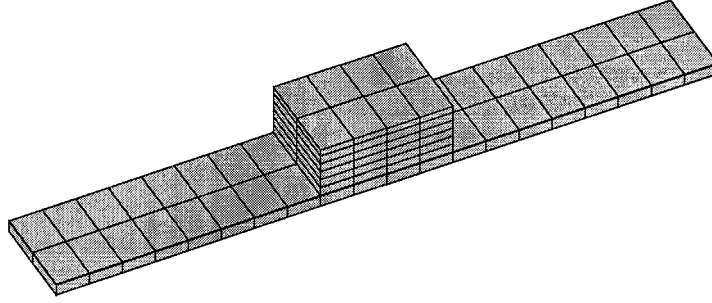


Figure 5. Validation model created for validation of thin, simply supported beam, optimal shape.

advantage of the diagonal symmetry of the plate structure. Thus, for a  $3 \times 3$  element plate, a structure that would require nine design variables can be reduced to requiring six design variables by taking advantage of diagonal symmetry. This diagonal symmetry condition is not applied within the optimization algorithm, but is taken into account in the interface between ABAQUS and NLPQL. In summary, the design constraints may be written:

$$V - V_0 \leq 0, \quad 0.254 \text{ mm} - (h_v)_i \leq 0 \quad (\text{for every element } i), \quad (8, 9)$$

where  $h_v$  is the height of the damping layer,  $V$ , is the volume of the damping material, and  $V_0$  is the initial volume of the damping material.

## 4. RESULTS

### 4.1. SIMPLY SUPPORTED BEAM

The first structure examined is a simply supported beam type structure, harmonically excited at its midpoint. The displacement results are normalized with the static midpoint displacement of the base structure, so the magnitude of the applied load is inconsequential.

The structure is modelled with continuum elements (ABAQUS types C3D20 and C3D27). All beam type structures examined have a length of 178 mm and a width of 25.4 mm. A thin ( $h_b = 3.18$  mm), and a thick ( $h_b = 15.2$  mm) base structure are investigated. Initial results are for the case where the volume of the damping layer is set to be equal to that of the base layer. In view of symmetry, only half of the structure is modelled with five elements through the length, and one element through the width of the base and constraining layers.

Figure 5 shows a fine mesh validation model corresponding to the optimum shape (created independently with 20-noded elements). The validation model shows good agreement with the optimization model. Table 2 gives the improvements in peak displacement and loss factor. The table shows a reduction of peak displacement by 92%

TABLE 2  
Results for simply supported beam,  $h_b = 3.18$  mm

	$\omega_d$ (Hz)	$w/w_{static}$	$\eta$
Uniform layer	195.52	1650	$6.00 \times 10^{-4}$
Optimized	176.63	131	$7.55 \times 10^{-3}$
Validation	175.99	125	$7.95 \times 10^{-3}$



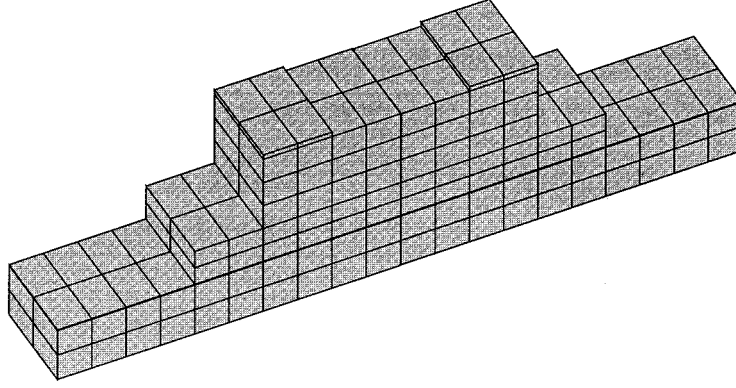


Figure 6. Validation model created for validation of thick, simply supported beam, optimal shape.

of the validation model over the uniform layer structure, where percentage reduction is defined by

$$\% \text{ reduction} = [w_u - w_o]/w_u, \quad (10)$$

$w_u$  and  $w_o$  denoting peak displacement of the uniform and optimal layers, respectively. An improvement of 1230% is seen for the loss factor, where percentage improvement is defined by

$$\% \text{ improvement} = [\eta_o - \eta_u]/\eta_u. \quad (11)$$

$\eta_u$  and  $\eta_o$  denoting the system loss factor of the uniform and optimal layers, respectively. Clearly, these numbers are quite attractive and provide a strong motivation to consider optimization.

By examining the deformed shape of the optimal structure, it was seen that a plane section through both layers in the undeformed structure does not remain plane when deformed. This indicates that the bending stress in the damping layer will not increase linearly away from the neutral axis. This result was confirmed by examining the stress contours in the damping layer. The bending stress diminished significantly towards the top of the damping layer. Additionally, the stress through the thickness of the damping layer was significant in the region near the base of the base structure. These two aspects of the optimal damping layer indicate that most traditional structural theories would not be able to adequately represent the laminate in the optimization process, as they assume both linear strain variation away from the neutral surface of the structure and negligible normal stress in the thickness direction. In fact, for “thick” structures, it is shown in Figure 1 that the loss factors, as determined by using plate elements, differ by as much as an order of magnitude from those calculated by using continuum elements.

TABLE 3

*Results for simply supported beam,  $h_b = 15.2$  mm*

	$\omega_d$ (Hz)	$w/w_{static}$	$\eta$
Uniform layer	909.9	15.0	0.0678
Optimized	928.0	3.55	0.410
Validation	960.0	3.96	0.315

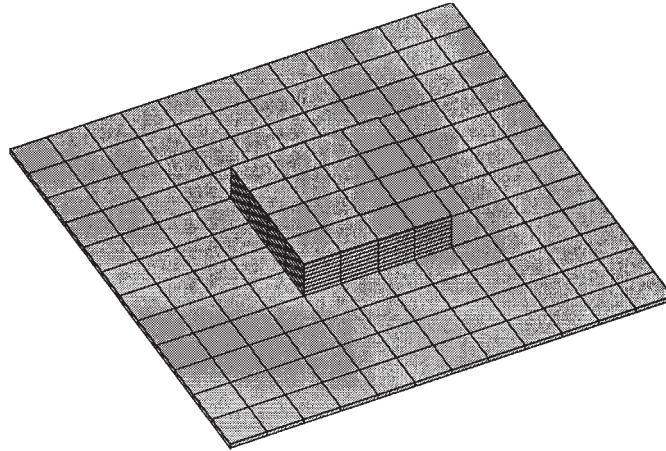


Figure 7. Validation model for optimal shape of thin, simply supported plate.

Figure 6 shows the fine mesh validation model for the thick beam. Table 3 gives the peak displacement and loss factor results. Significant improvements are again seen. There is a 74% improvement in displacement and a 365% improvement in the loss factor.

#### 4.2. SIMPLY SUPPORTED PLATE

Simply supported plates harmonically loaded at the center are now examined. Again, the displacement results are normalized, such that the load magnitude is inconsequential. The normalization factor is the midpoint displacement due to a load at the plate's center, which can be found in reference [26]. Again C3D20 and C3D27 element types are used. The plate is taken to be square, 305 mm to a side. Both thin ( $h_b = 3.18$  mm) and thick ( $h_b = 15.2$  mm) base structures are investigated. In both cases, the volume of the damping layer is set to be equal to that of the base layer. Only one-quarter of the plate is modelled in view of symmetry. The base structure is modelled with nine elements, in a  $3 \times 3$  configuration.

The fine mesh optimal shape is shown in Figure 7 with corresponding performance measures shown in Table 4. The validation model was created independently with 20-noded continuum elements (type C3D20). The validation model agrees quite well with the optimized model, with 2% or less difference in the midpoint displacement and loss factor results between the two models.

The optimized model shows a 97% decline in its midpoint displacement from the uniform layer model, and a 3830% improvement in the system loss factor. The improvements are on the same order as was seen for the beam.

Similar results for the thick base structure are given in Figure 8 and Table 5. Again, results from the validation model are quite close to the optimized model, within 4% both

TABLE 4

*Results for simply supported plate,  $h_b = 3.18$  mm*

	$\omega_d$ (Hz)	$w/w_{static}$	$\eta$
Uniform layer	140.09	1840	$4.78 \times 10^{-4}$
Optimized	112.15	47.9	$1.88 \times 10^{-2}$
Validation	111.04	48.9	$1.90 \times 10^{-2}$

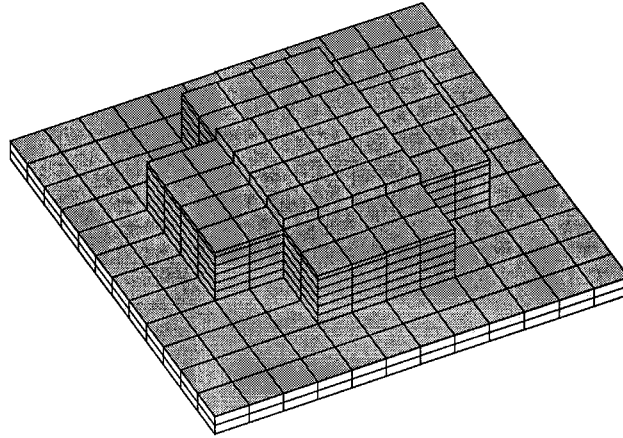


Figure 8. Validation model for optimal shape of thick, simply supported plate.

in the peak displacement and the loss factor. The optimized model shows a 92% reduction in displacement and a 1740% increase in the system loss factor over the uniform layer model. Again, these numbers are quite attractive, and consistent with those seen in optimizing the damping layer on the simply supported beam.

#### 4.3. FULLY CLAMPED PLATE

A natural question to ask is whether one would also obtain such substantial gains for clamped plates, and this issue is addressed in the sequel. The dimensions of the plate are

TABLE 5

*Results for simply supported plate,  $h_b = 15.2$  mm*

	$\omega_d$ (Hz)	$w/w_{static}$	$\eta$
Uniform layer	649.15	33.0	0.0278
Optimized	541	2.70	0.512
Validation	543	2.75	0.531

TABLE 6

*Results for fully clamped plate,  $h_b = 3.18$  mm*

	$\omega_d$ (Hz)	$w/w_{static}$	$\eta$
Uniform layer	291.553	1840	$7.73 \times 10^{-4}$
Optimized	209.3	20.6	$4.58 \times 10^{-2}$
Validation	189.3	27.5	$4.15 \times 10^{-2}$

TABLE 7

*Results for fully clamped plate,  $h_b = 15.2$  mm*

	$\omega_d$ (Hz)	$w/w_{static}$	$\eta$
Uniform layer	1234.7	11.8	0.0702
Optimized	1217	2.13	0.774
Validation	1076	2.38	0.699

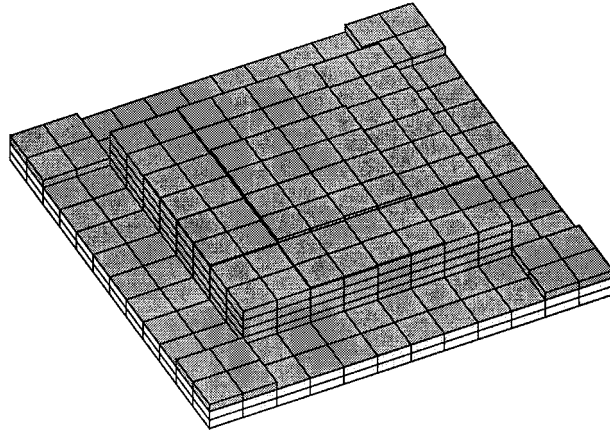


Figure 9. Validation model for optimal shape of thick, fully clamped plate.

taken to be the same as those of the simply supported plate. The displacement results were normalized by the static peak displacements, obtained from a finite element analysis.

Table 6 gives the results for a thin clamped plate. The optimal shape turned out to be identical to that shown in Figure 8 for the thin, simply supported plate. Again, dramatic benefits are seen over the uniform layer, with 98% peak displacement reduction and 5270% system loss factor improvement.

Table 7 shows results for the fully clamped thick plate, and Figure 9 shows the optimized shape validation model. Improvements of 80% and 896% in the peak displacement and system loss factor, respectively, are seen.

#### 4.4. PARAMETER STUDIES

In the previous section, it was demonstrated that optimizing the shape of the damping layer of an unconstrained laminate yields remarkable improvement in the peak

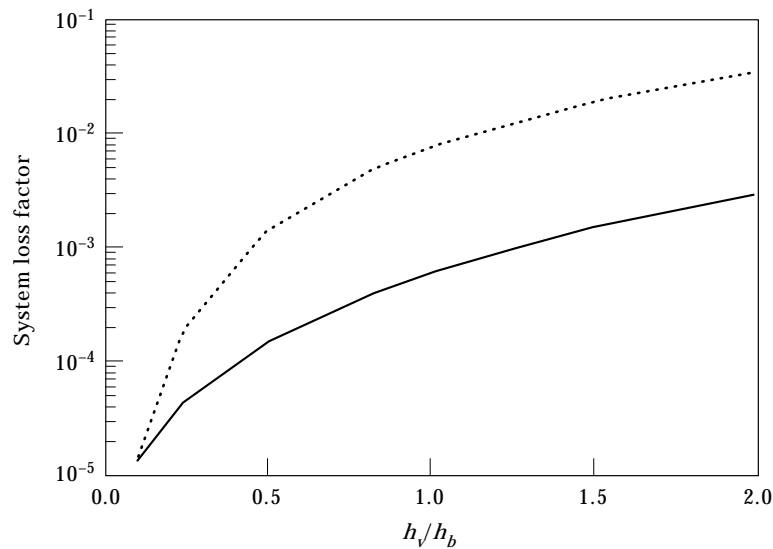


Figure 10. Plot of system loss factor versus  $h_v/h_b$  for uniform (—) and optimized (····) damping layers,  $h_b = 3.18$  mm.

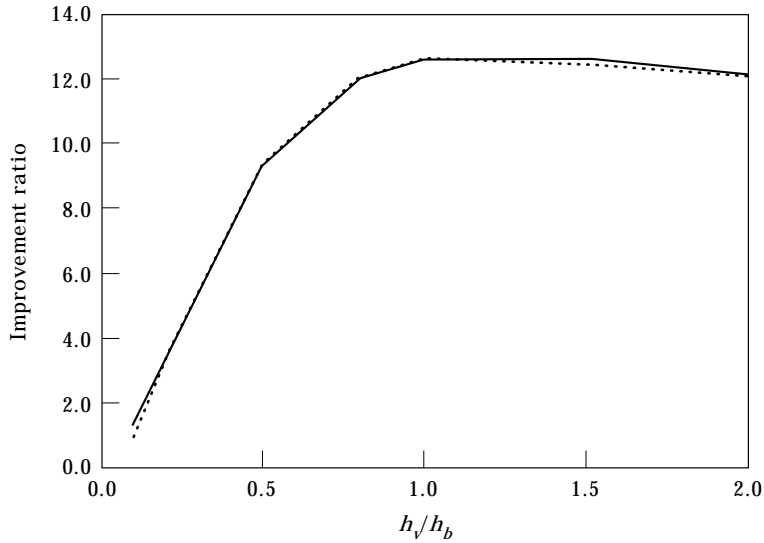


Figure 11. Plot of displacement (—) and system loss factor (····) improvement ratio versus  $h_v/h_b$ ,  $h_b = 3.18$  mm.

displacement and the system loss factor for a variety of different configurations. In each of those configurations, the volume of the damping layer was equal to that of the base structure. Consideration will now be given to how much improvement in performance is possible for different damping layer volumes. Optimization studies are performed for both thin and thick structures for damping layer volumes ranging from 10 to 200% of the volume of the base beam. The volume ratio is given by  $h_v/h_b$ , where  $h_v$  denotes the height of the original uniform damping layer and  $h_b$  denotes the height of the base layer.

Figure 10 shows how the system loss factor varies with  $h_v/h_b$  for a damping layer on a thin base for both the uniform and optimized damping layers. (Note that for the optimized structures the  $h_v/h_b$  ratio represents the initial height that led to the optimized shape). Some of the optimal shapes (only half the beams are shown) along with resonance frequencies and loss factors are given in Table 8.

TABLE 8  
Results for parameter study,  $h_b = 3.18$  mm

$h_v/h_b$	$\omega_d$ uniform layer	$\omega_d$ optimized	$\eta$ uniform layer	$\eta$ optimized	Optimal shape
0.1	223.08	222.39	$1.38 \times 10^{-5}$	$1.40 \times 10^{-5}$	
0.5	209.48	198.30	$1.49 \times 10^{-4}$	$1.40 \times 10^{-3}$	
2.0	174.31	147.26	$2.87 \times 10^{-3}$	$3.45 \times 10^{-2}$	

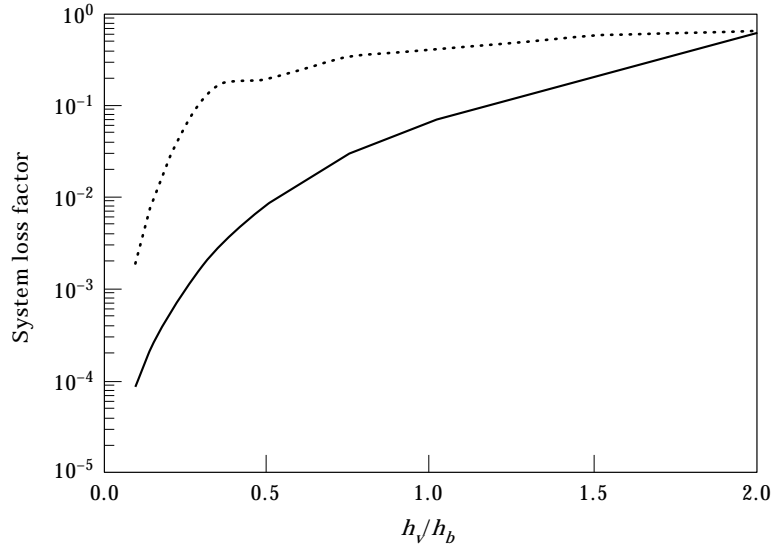


Figure 12. Plot of system loss factor versus  $h_v/h_b$  for uniform (—) and optimized (····) damping layers,  $h_b = 15.2$  mm.

Figure 11 shows plots of the displacement improvement ratio ( $w_u/w_o$ ) and the system loss factor improvement ratio ( $\eta_o/\eta_u$ ) as a function of the ratio  $h_v/h_b$  for  $h_b = 3.18$  mm. Note that the improvements obtained initially increase as the volume of the damping layer increases, but eventually reach a peak value of about 12.5 and begin to decline slightly. An agent contributing to the decline in the loss factor is the role of the damped natural frequency. As Table 8 shows, as  $h_v/h_b$  increases, the difference in the damped natural frequency of the uniform and optimal layers increases. These frequencies lie in a region where the damping material loss factor and moduli decrease with decreasing frequency.

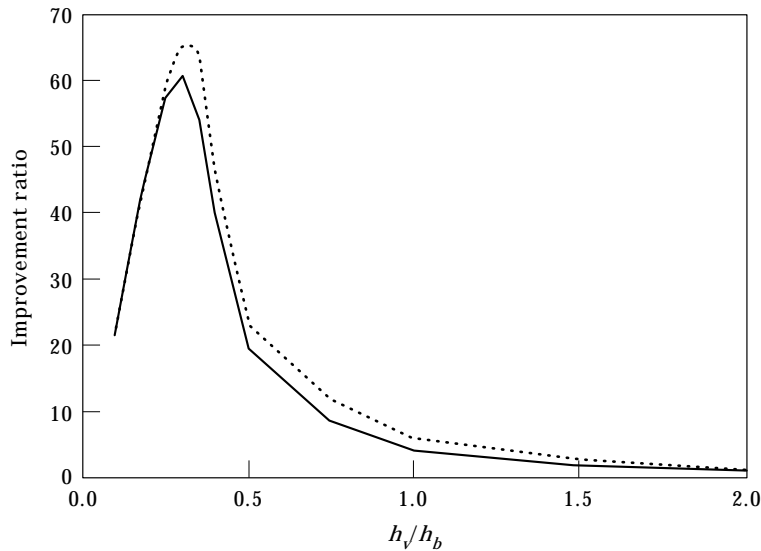



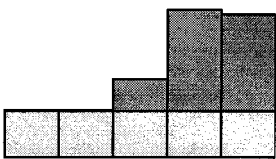
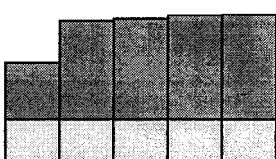


Figure 13. Plot of displacement (—) and system (····) loss factor improvement ratio versus  $h_v/h_b$ ,  $h_b = 15.2$  mm.

TABLE 9  
*Results for parameter study,  $h_b = 15.2$  mm*

$h_v/h_b$	$\omega_d$ uniform layer	$\omega_d$ optimized	$\eta$ uniform layer	$\eta$ optimized	Optimal shape
0.1	1053.9	1040.3	$8.83 \times 10^{-5}$	$2.00 \times 10^{-3}$	
0.4	1002.4	1011.2	$4.12 \times 10^{-3}$	0.189	
0.5	985.9	983.8	$8.38 \times 10^{-3}$	0.194	
1.0	909.8	928.0	0.0679	0.410	
2.0	800.0	889.0	0.621	0.656	

Thus, anything that reduces the damped natural frequency will reduce the damping material loss factor and stiffness which will result in a reduction of the system loss factor.

Note that the improvement ratios are almost identical for displacements and loss factors. This would tend to indicate that there is a good correlation between these two measures

TABLE 10  
*Results for simply supported beam,  $h_b = 3.18$  mm; constant viscoelastic properties for the damping material, taken at the natural frequency of the equivalent elastic laminated beam*

	$\omega_d$ (Hz)	$w/w_{static}$	$\eta$
Uniform layer	195.52	1650	$5.98 \times 10^{-4}$
Optimized	176.66	134	$7.36 \times 10^{-3}$

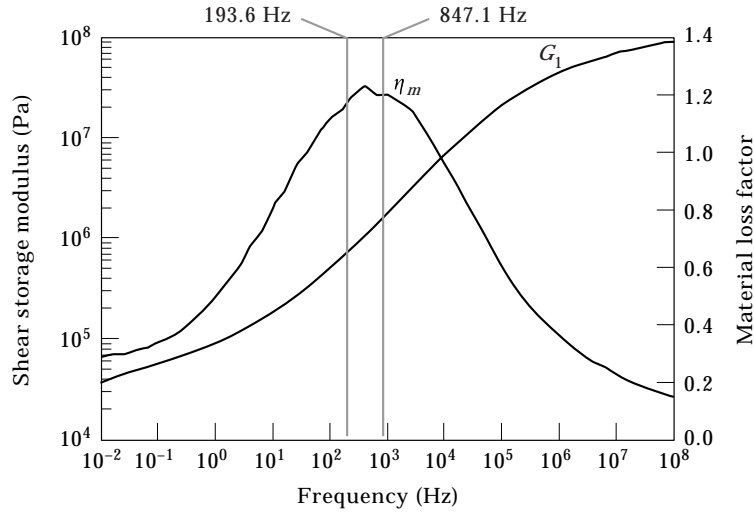


Figure 14. Shear storage modulus and material loss factor for damping material; frequencies of constant property models shown.

of damping in the structure. It was argued previously that, although the system loss factor is a global measure of a laminate's damping performance, the peak displacement is an adequate measure. This conjecture is strongly supported by the good correlation.

Figure 12 shows the loss factor as a function of  $h_v/h_b$  for the thick beam and Figure 13 shows the improvement ratios as a function of  $h_v/h_b$  for the thick beam. As in the thin beam, the improvement ratio reaches a maximum and then decreases as the volume of the damping layer increases. However, this drop off after the maximum value is reached is more dramatic for the thick beam than for the thin. The reasons for this are explained in the sequel.

Table 9 gives the natural frequencies and system loss factors for some of the uniform and optimal shapes. Also shown are the corresponding optimal shapes. It can be seen that, for small values of  $h_v/h_b$ , all of the damping material moves to the center of the beam. But, as  $h_v/h_b$  reaches a value of 0.4, a small amount of damping material is placed at the element adjacent to the element in the center of the beam for the optimal shape. This is the point at which the improvement ratios reach their peak and begin to decline. This trend continues, such that, as  $h_v/h_b$  increases, more material is placed on elements away from the center of the beam. Thus, as  $h_v/h_b$  increases, the optimal shape tends to look more like the uniform layer, and the improvement ratio tends toward a value of one.

Some insight into the cause of the diminishing improvement ratios can be found by closer examination of the system loss factor in Figure 12. It can be seen that, as  $h_v/h_b$  increases,  $\eta$  initially increases significantly for the optimal shape, but then levels off. When measured by half power bandwidth,  $\eta$  can achieve a maximum value of 1.0 for cases of viscous damping [27]. Thus, there is a limit to the amount of increase that the system loss factor can experience. For viscoelastic damping treatments,  $\eta$  cannot exceed the material loss factor. The material loss factor for this particular material has a maximum value of 1.23, and is about 1.2 in the frequency range 800–1100 Hz that is of concern here. Both the uniform layer structure and the optimal could not surpass this value as the volume of damping material increases. Thus, the improvement ratio should ultimately go to one as both the uniform and optimal structures approach this limit. Figure 12 shows a region where the optimal layer begins to show very little improvement (around  $h_v/h_b = 0.4$ ), but



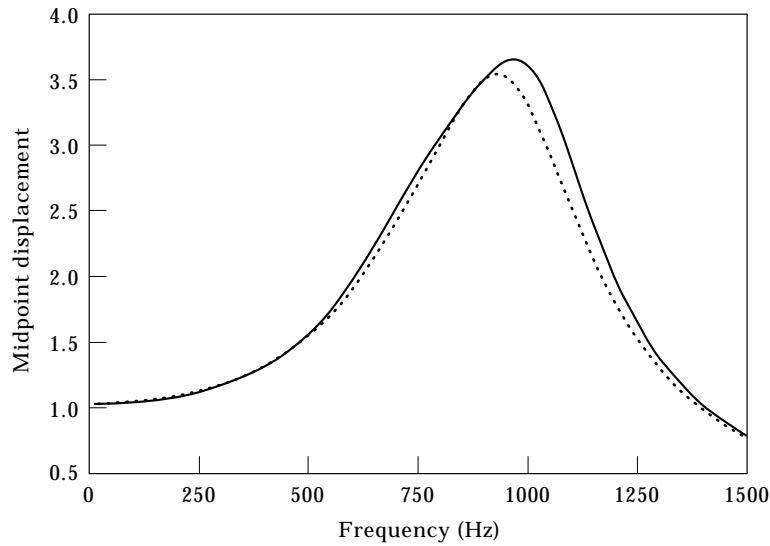


Figure 15. Response of optimized thick beam; viscoelastic material with constant properties (—) and frequency varying properties (····).

the uniform layer continues to show marked improvement. This is the region where the improvement ratio falls off dramatically.

#### 4.5. SIGNIFICANCE OF FREQUENCY DEPENDENT VISCOELASTIC PROPERTIES

Many difficulties are involved in incorporating realistic frequency dependence of viscoelastic material properties into an analytic formulation. It is not difficult to incorporate a frequency dependence that is based on a parametric model (such as Maxwell or Kelvin–Voigt models). However, these models are rarely useful for modelling real viscoelastic materials over any significant frequency range. Some difficulties are also involved in incorporating realistic frequency dependence of viscoelastic material properties into a finite element formulation for a damped laminate. The Modal Strain Energy Method, which is frequently used to find natural frequencies and system loss factors for damped laminates, cannot easily include frequency dependent properties. Also, many commercial finite element codes do not have a straightforward technique for modelling a material with frequency dependent properties. As a result, many analytic solutions, as well as many finite element solutions, make the assumption that the viscoelastic properties are constant with frequency. Several previous optimization studies of unconstrained layer plates [11, 16, 17] have made the assumption of constant damping properties. Thus, it is worthwhile to examine the effect of this assumption on the optimization results.

TABLE 11

*Results for simply supported beam,  $h_b = 15.2$  mm; constant viscoelastic properties for the damping material, taken at the natural frequency of the equivalent elastic laminated beam*

	$\omega_d$ (Hz)	$w/w_{static}$	$\eta$
Uniform layer	909.1	14.5	0.0678
Optimized	919.0	3.59	0.453

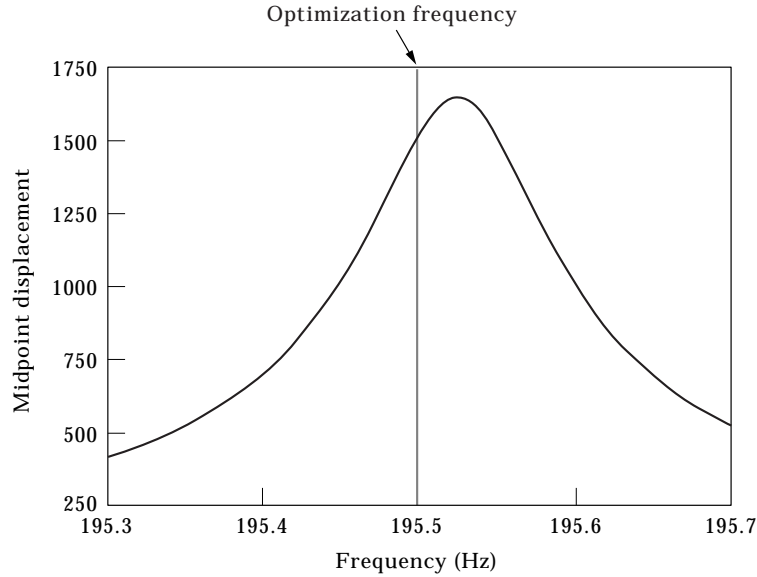


Figure 16. Normalized midpoint displacement of uniform layer, simply supported beam,  $h_b = 3.18$  mm.

The question arises: at what frequency should the constant properties be taken? It would be most natural to take them at the damped resonance frequency of the uniform layer structure. However, the damped resonance frequency cannot be found without knowing the properties of the damping layer. Thus, the damping material properties will be taken at the natural frequency of an equivalent elastic structure, where the viscoelastic damping is ignored. This frequency can easily be found by an analytic or a finite element solution. The stiffness of the equivalent elastic damping layer is still not known, but, as it is several orders of magnitude less than that of the base structure (aluminum in this case), it should not play a significant role in the magnitude of natural frequency. The density of the damping material is about one-third that of aluminum, however, so it will have an influence on the resonance frequency of the composite. Figure 14 shows the shear storage modulus and material loss factor of the viscoelastic material, giving the frequencies (for thin and thick beams) at which the constant properties are taken for this study.

TABLE 12

*Results for simply supported beams,  $h_b = 3.18$  mm; minimize displacement at one fixed frequency (195.5 Hz)*

	$\omega_d$ (Hz)	$W_{195.5 \text{ Hz}}/W_{static}$	$W_{\omega_d}/W_{static}$	$\eta$
Uniform layer	195.52	1520	1650	$4.78 \times 10^{-4}$
Optimized	223.83	4.18	93 200	$1.06 \times 10^{-5}$

TABLE 13

*Results for simply supported beams,  $h_b = 3.18$  mm; minimize displacement at one fixed frequency (195.5 Hz), new optimization parameters*

	$\omega_d$ (Hz)	$W_{195.5 \text{ Hz}}/W_{static}$	$W_{\omega_d}/W_{static}$	$\eta$
Uniform layer	195.52	1520	1650	$4.78 \times 10^{-4}$
Optimized	176.63	4.38	131	$7.55 \times 10^{-3}$

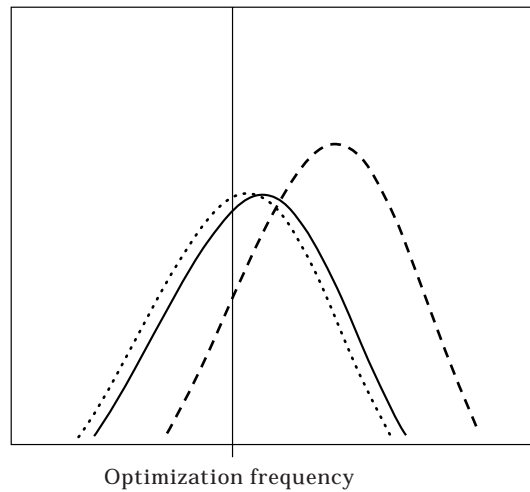


Figure 17. Frequency response with a small finite difference step size: (—), uniform layer response; (····), response from first finite difference; (---), response after one iteration.

The structures examined are the simply supported beams that were examined previously. For the thin beam, eigenvalue analysis showed the first natural frequency (in bending) of the equivalent elastic system to be 193.6 Hz. Table 10 shows the results of optimization with constant properties for the viscoelastic material (taken at 193.6 Hz). The optimal shape result in this case is identical to that of the optimization with frequency dependent properties—all of the damping material is placed in the center of the beam. The peak displacement shows a 92% decline, while the system loss factor shows a 1130% improvement over the uniform layer. This compares to a 1160% improvement in the system loss factor for the optimized model with frequency dependent properties, a 2.6% difference. So, in this case, it appears that the constant viscoelastic properties assumption has negligible effect.

Table 11 shows the optimization results of the thick beam with constant properties for the viscoelastic material (taken at 847.1 Hz, found by eigenvalue analysis). The optimal

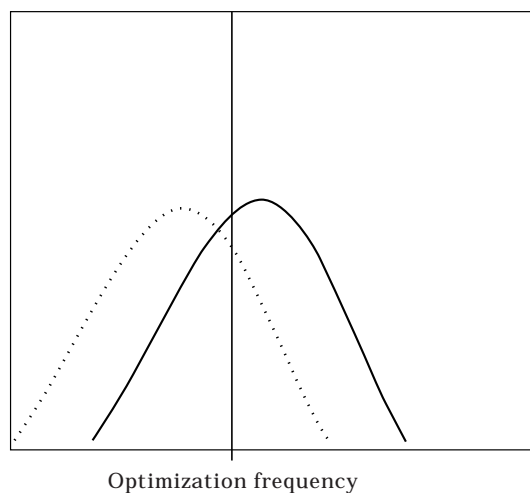


Figure 18. Frequency response with a large finite difference step size: (—), uniform layer response; (····), response from first finite difference.

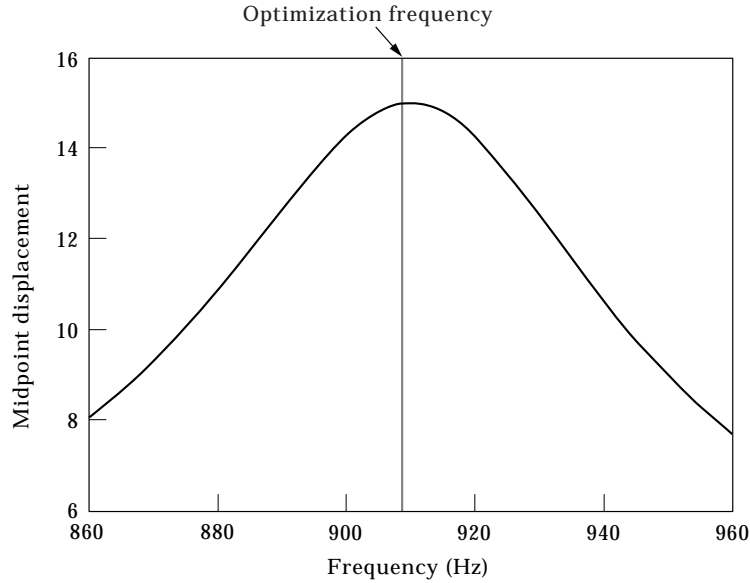


Figure 19. Normalized midpoint displacement of uniform layer, simply supported beam,  $h_b = 15.2$  mm.

shape result in this case is very similar to that of the optimization with frequency dependent properties. The peak displacement shows a 75% decline, while the system loss factor shows a 568% improvement over the uniform layer. This compares to a 515% improvement in the system loss factor for the optimized model with frequency dependent properties. The improvement for the constant properties optimal shape is 10% greater than for the frequency dependent properties optimal shape. This difference could be significant for some applications. It is worth noting that, for the thin beam, the constant properties optimal shape shows *less* improvement than the varying properties shape, while in this case, it shows *more* improvement. Thus, no generalization may be made about the direction of the error in assuming constant properties.

The reason for the difference between the constant frequency and frequency varying results is likely to be the values of the material properties. At 847.1 Hz, the frequency at which the properties are taken for the constant properties optimization, the material loss factor is a bit higher than at 928 Hz, which is the resonance frequency for the varying frequency optimal shape. The system loss factor is dependent upon the material loss factor, as well as the stiffness and the geometry of the composite's constituents. It is intuitively clear that the system loss factor will increase as the material loss factor increases, but it is not clear how the system loss factor will vary with damping layer stiffness. It would appear that, in this case, a lower damping layer storage modulus leads to a higher system loss factor. One final consideration is that, as the system loss factor is calculated by half

TABLE 14

*Results for simply supported beams,  $h_b = 15.2$  mm; minimize displacement at one fixed frequency (909.0 Hz)*

	$\omega_d$ (Hz)	$W_{195.5 \text{ Hz}}/W_{static}$	$W_{\omega_d}/W_{static}$	$\eta$
Uniform layer	909.8	15.0	15.0	0.0678
Optimized	1005	3.33	3.81	0.317

power bandwidth, it is dependent on the response over a large range of frequencies. In this case, the half power points occur over a frequency range of more than 300 Hz. Thus, when realistic (frequency varying) viscoelastic properties are assumed, the viscoelastic material properties vary significantly over this range, and this will in turn affect the loss factor result. This effect is seen in Figure 15. The shape used for this comparison is the optimal shape of the frequency varying model with  $h_v/h_b = 1$ . In this case, the frequency dependent properties result has a lower half power bandwidth (and thus system loss factor) than the constant properties result. It is not intuitively clear, however, whether this effect will always make the system loss factor higher or lower. In this case, the material loss factor for the frequency varying case is lower over most of the frequency range of concern; however, the system loss factor is a function, not only of the material loss factor, but also of the material stiffness, which also varies in this region. Thus, no clear generalization can be made.

#### 4.6. OPTIMIZATION AT ONE FREQUENCY

The approach of the studies up to this point has been to minimize the peak displacement at the damped resonance frequency, which changes with each design change. Several studies in the optimization of laminated structures (references [9, 12], for example) have examined minimizing the displacement of the structure at one fixed frequency just below the resonance frequency. It is shown below that this objective may produce undesirable side effects. The same two models (thin beam and thick beam) are examined as in the studies above.

Figure 16 shows the frequency response of the first mode for the thin simply supported beam, and also shows the frequency at which the displacement is minimized (195.5 Hz). Table 12 shows the results of optimization. It can be seen that, although the displacement at 195.5 Hz is reduced by 99.7% for the optimized structure, the displacement at the new natural frequency actually increases by 5550%. This indicates that the major cause of the reduction in displacement at 195.5 Hz is movement of the resonance peak away from this frequency, rather than improved damping characteristics. This is verified by the fact that each of the damping layer heights went to their minimum values in the optimization process. Reducing the damping layer height decreases the damping in the system, but it also decreases the mass of the composite, thus giving it a higher resonance frequency.

If a few of the optimization parameters are changed, however, (namely, the objective function scaling factor and the finite difference step size), a different optimal shape is obtained. This new optimal shape is the same as is shown in Figure 5 using the previous optimization procedure. That is, it is the same shape as was obtained by minimizing the peak displacement. Table 13 gives the results associated with this shape. Both the response at 195.5 Hz, and the response at the new damped natural frequency show tremendous improvement.

It should be emphasized again that the optimization algorithm only guarantees a local optimum. This explains the possibility of two significantly different optimal designs associated with one problem. Each is a local optimum. It should also be emphasized that, in both cases, typical values were chosen for the parameters in question.

The reason that different optimization parameters, particularly the finite difference step size, cause this bifurcation is as follows. The optimally shaped beam that has the favorable damping properties has a natural frequency below that of the uniform layer. As the frequency under consideration (195.5 Hz) is below the uniform layer natural frequency, a small finite difference step size will have the tendency to cause the natural frequency to be higher. This is because a small finite difference step size means that there are small increments in the damping layer heights to obtain gradient information, and a structural

change that causes the resonance peak to move slightly lower means an increase in displacement. This effect is demonstrated below in Figure 17. Thus, the main means of decreasing the displacement at the given frequency is to cause the natural frequency to be higher, and this is accomplished by removing damping material. On the other hand, if the finite difference step size is relatively large, then the increment in the damping layer height is large enough to lower the resonant peak to an extent that the displacement at that increment is less. Thus, the resonant peak is free to move to a lower value. This effect is demonstrated in Figure 18. The natural frequency is moved to a lower value by placing the damping material in the center of the beam, where the damping properties are maximized.

The frequency response about the first resonance of the thick beam is shown in Figure 19. Also shown is the frequency (909 Hz) at which the midpoint displacement is minimized, just below resonance. Table 14 gives the results for this optimization. In this case, the midpoint displacement at 909 Hz is reduced by 77.8%, and the midpoint displacement at the new resonance is also reduced by 74.6%. This structure is not sensitive to changes in the optimization parameters in the way that the thin simply supported beam is. The reason for this is that the structure optimized by minimizing the peak displacement has a higher resonance frequency than the uniform layer structure. Thus, both a small finite difference step size and a large finite difference step size will serve to move the resonance frequency higher, which is accomplished by moving the damping material towards the center of the beam. It should be noted that the optimal shape in this case differs slightly from the optimal shape obtained from minimizing the peak displacement, and the loss factor improvement given in Table 14 is not as great as that given previously. But it is most notable that, in this case, minimizing the displacement at one frequency improves the performance at the new resonance frequency as well.

Minimizing the displacement of a structure at a given frequency may be useful in cases when that structure will be operating over a narrow frequency range. It is seen in every case examined here that the displacement at the selected frequency is reduced significantly. However, if it is possible that the structure will stray outside of that narrow frequency range, optimizing at one frequency should be done with caution. It has been shown here that traditional optimization techniques can cause the performance of the structure at the new natural frequency to be significantly worse than the initial, uniform shape.

## 5. CONCLUSIONS

These studies show that significant improvement is possible in the optimization of the shape of an unconstrained damping layer. For a given amount of damping material, the system loss factor shows order of magnitude improvements in most cases, and the peak displacement may be reduced by as much as 98%. The results are quite robust. Substantial improvement was observed for many different structures and many different boundary conditions. The current studies also show that structural elements are not useful in the optimization of many unconstrained damped laminates. The reasons for this are that plane sections do not remain plane in the structure, and the normal stress through the thickness is not negligible, as most structural theories assume.

The shape of an unconstrained damping layer was also optimized for a wide range of damping layer volumes. The optimization process showed great robustness, with the optimized damping layer achieving significantly greater damping effectiveness than the uniform damping layer in all cases. For the thick beam, however, the amount of improvement peaked as the damping material volume reached 30% of the base layer volume, and decreased as the damping layer volume increased. This is, in part, because

the system loss factor for the uniform layer became large enough that the same magnitude of improvement could not be achieved.

It was also shown that minimizing the displacement at one given frequency near resonance, rather than at the resonance frequency, should be done with care. Using typical values for the optimization parameters, this may result in a significantly worse global design.

Additionally, it is shown that assuming constant (rather than frequency varying) viscoelastic properties causes only minor differences in the optimization results.

#### ACKNOWLEDGMENT

The authors would like to acknowledge and thank the 3M company of Minneapolis, Minnesota for providing the data for Figure 2.

#### REFERENCES

1. B. C. NAKRA 1976 *Shock and Vibration Digest* **8**, 3–12. Vibration control with viscoelastic materials.
2. B. C. NAKRA 1981 *Shock and Vibration Digest* **13**, 17–20. Vibration control with viscoelastic materials—II.
3. B. C. NAKRA 1984 *Shock and Vibration Digest* **16**, 17–22. Vibration control with viscoelastic materials—III.
4. D. ROSS, E. E. UNGAR and E. M. KERWIN, JR. 1959 in *Structural Damping* (J. E. Ruzicka, editor), section 3. ASME. Damping of plate flexural vibrations by means of viscoelastic laminae.
5. S. J. HWANG, R. F. GIBSON and J. SINGH 1992 *Composites Science and Technology* **43**, 159–169. Decomposition of coupling effects on damping of laminated composites under flexural vibration.
6. R. PLUNKETT and C. T. LEE 1970 *The Journal of the Acoustical Society of America* **48**, 150–161. Length optimization for constrained viscoelastic layer damping.
7. R. LUNDÉN 1979 *Journal of Sound and Vibration* **66**, 25–37. Optimum distribution of additive damping for vibrating beams.
8. R. LUNDÉN 1980 *Journal of Sound and Vibration* **72**, 391–402. Optimum distribution of additive damping for vibrating frames.
9. T. LEKSZYCKI and N. OLHOFF 1981 *The Journal of Structural Mechanics* **9**, 363–387. Optimal design of viscoelastic structures under forced steady-state vibration.
10. B. L. PIERSON 1986 *Computer Methods in Applied Mechanics and Engineering* **57**, 37–49. An optimal control approach to the design of vibrating elastic-viscoelastic sandwich beams.
11. A. YILDIZ and K. STEVENS 1985 *The Journal of Sound and Vibration* **103**, 183–199. Optimum thickness distribution of unconstrained viscoelastic layer treatments for plates.
12. T.-C. LIN and R. A. SCOTT 1987 *Proceedings of the 58th Shock and Vibration Symposium, Huntsville, Alabama* **1**, 395–409. Shape optimization of damping layers.
13. J. M. LIFSHTZ and M. LEIBOWITZ 1987 *International Journal of Solids and Structures* **23**, 1027–1034. Optimal sandwich beam design for maximum viscoelastic damping.
14. D. J. MEAD and S. MARKUS 1969 *Journal of Sound and Vibration* **10**, 163–175. The forced vibration of a three-layer, damped sandwich beam with arbitrary boundary conditions.
15. P. HAJELA and C.-Y. LIN 1991 *Applied Mechanics Review* **44**, S96–S106. Optimal design of viscoelastically damped beam structures.
16. P. K. ROY and N. GANESAN 1993 *Computers and Structures* **49**, 473–480. Dynamic studies on plates with unconstrained layer treatment.
17. P. K. ROY and N. GANESAN 1996 *Journal of Sound and Vibration* **195**, 417–427. Dynamic studies on beams with unconstrained layer treatment.
18. A. LUMSDAINE and R. A. SCOTT 1995 *Proceedings of the ASME 15th Biennial Conference on Mechanical Vibration and Noise, Boston, MA*. Shape optimization of unconstrained beam and plate damping layers.
19. A. LUMSDAINE and R. A. SCOTT 1996 *NOISE-CON 96, National Conference on Noise Control Engineering, Seattle, WA*, 509–514. Optimal design of unconstrained damping layers using continuum finite elements.
20. A. LUMSDAINE and R. A. SCOTT 1997 *Proceedings of the Symposium on Vibroacoustic Methods in Processing and Characterization of Advanced Materials and Structures at the 1997 ASME*

- International Mechanical Engineering Congress and Exposition, Dallas, TX*. Parameter studies in the optimal design of unconstrained beam damping layer treatments.
21. A. LUMSDAINE 1996 *Ph.D. Dissertation, The University of Michigan*. Optimal design of damped laminated structures.
  22. Z. RIGBI 1967 *Applied Polymer Symposia* **5**, 1–8. The value of Poisson's ratio of viscoelastic materials.
  23. D. J. EWINS 1984 *Modal Testing: Theory and Practice*. Letchworth, U.K.: Research Studies Press.
  24. K. SCHITTKOWSKI 1986 *Annals of Operations Research* **5**, 485–500. NLPQL: a FORTRAN subroutine for solving constrained non-linear programming problems.
  25. A. K. LALL, B. C. NAKRA and N. T. ASNANI 1983 *Engineering Optimization* **6**, 197–205. Optimum design of viscoelastically damped sandwich panels.
  26. E. VOLTERRA and J. H. GAINES 1971 *Advanced Strength of Materials*. Englewood Cliffs, NJ: Prentice Hall.
  27. A. D. NASHIF, D. I. G. JONES and J. P. HENDERSON 1985 *Vibration Damping*. New York: John Wiley and Sons. See pp. 133–134.